

Synthesis, Characterization and OFET Properties of Amphiphilic Mixed (Phthalocyaninato)(porphyrinato)europium(III) Complexes

Pan Ma,^[a] Yanli Chen,^[b] Ning Sheng,^[a,c] Yongzhong Bian,^[a] and Jianzhuang Jiang*^[a]

Keywords: Phthalocyanines / Porphyrinoids / Rare earths / Sandwich complexes / OFETs (organic field-effect transistors)

Amphiphilic mixed (phthalocyaninato)(porphyrinato)europium(III) triple-decker complexes $\text{Eu}_2[\text{Pc}(\text{15C5})_4]_2[\text{T}(\text{C}_{10}\text{H}_{21})_4\text{P}]$ (**1**) and $\text{Eu}_2[\text{Pc}(\text{15C5})_4]_2[\text{TPOPP}]$ (**2**) [$\text{H}_2\text{Pc}(\text{15C5})_4 = 2,3,9,10,16,17,23,24$ -tetrakis(15-crown-5)phthalocyanine; $\text{H}_2\text{T}(\text{C}_{10}\text{H}_{21})_4\text{P} = \text{meso-5,10,15,20-tetra-}n\text{-decylporphyrin}$, $\text{H}_2\text{TPOPP} = \text{meso-5,10,15,20-tetrakis(4-pentyloxyphenyl)porphyrin}$] were designed and synthesized by the raise-by-one-story method. These novel sandwich triple-decker complexes were characterized by a wide range of spectroscopic methods, and they were also electrochemically studied. Highly ordered films were fabricated by the Langmuir–

Blodgett (LB) technique into organic field-effect transistors (OFETs). The devices display good OFET performance with a carrier mobility in the range $0.03\text{--}0.78\text{ cm}^2\text{V}^{-1}\text{s}^{-1}$. As expected, the devices show a low threshold voltage range from -1.19 to -4.34 V . The mobility of compound **1** reaches $0.78\text{ cm}^2\text{V}^{-1}\text{s}^{-1}$, which is the highest value so far achieved for LB film-based OFETs, as a result of the narrow energy gap (1.04 eV) of this compound.

(© Wiley-VCH Verlag GmbH & Co. KGaA, 69451 Weinheim, Germany, 2009)

Introduction

Research on organic semiconductors for organic field-effect transistors (OFET) has made great progress since the first report on OFETs in 1986.^[1] In comparison to their inorganic counterparts, organic optoelectronic devices possess many unique advantages such as light weight, low cost, flexibility and low-temperature device fabrication.^[2] Phthalocyanines (Pc) and porphyrins (Por) as the promising active materials for OFETs have had wide range of applications for a long time.^[3] In addition to their intrinsic molecular and electronic properties, the influence of substrate temperature and substrate treatment methods on the characteristics of OFETs was revealed for the vacuum-deposited copper phthalocyanine thin-film transistor.^[4] Thus far, the single crystal CuPc-based OFET was reported to show carrier mobility as high as $1.0\text{ cm}^2\text{V}^{-1}\text{s}^{-1}$.^[5] Noh and coworkers investigated epitaxially grown films of (octaethyl)(porphyrinato)platinum with a mobility of $10^{-4}\text{ cm}^2\text{V}^{-1}\text{s}^{-1}$.^[6] A spin-coated film of benzoporphyrin was reported to show a carrier mobility around $10^{-2}\text{ cm}^2\text{V}^{-1}\text{s}^{-1}$.^[7] Checcoli et al. reported the use of 5,10,15,20-tetraphenylporphyrin as a *p*-type organic semiconductor with a mobility ranging from

0.007 to $0.012\text{ cm}^2\text{V}^{-1}\text{s}^{-1}$.^[8] Langmuir–Blodgett (LB) films of substituted monomeric phthalocyanine and bis(phthalocyaninato) rare-earth complexes were revealed to show mobilities in the range of 10^{-6} to $10^{-3}\text{ cm}^2\text{V}^{-1}\text{s}^{-1}$.^[9,24] Nevertheless, the LB films of amphiphilic heteroleptic tris(phthalocyaninato) rare-earth triple-decker complexes displayed good OFET characteristics with high carrier mobility for holes of $0.24\text{--}0.60\text{ cm}^2\text{V}^{-1}\text{s}^{-1}$.^[10]

Since the end of last century, mixed (phthalocyaninato)(porphyrinato) rare-earth analogues have received increasing attention partly because the individual chromophores display very different optical and redox properties, which facilitate the study of π – π interactions and the extent of hole delocalisation.^[11] Mixed (phthalocyaninato)(porphyrinato) rare-earth triple-decker complexes were also attractive for their potential use in information storage as a result of their large number of redox states, reversible electrochemistry and relatively low oxidation potentials.^[12] These mixed (phthalocyaninato)(porphyrinato) rare-earth triple-decker complexes are expected to be good organic semiconducting materials for OFET devices owing to their common molecular electronic structure with tris(phthalocyaninato) rare-earth triple-decker complexes.^[10]

In this paper, we describe the design, synthesis, spectroscopic and electrochemical properties of two novel amphiphilic mixed (phthalocyaninato)(porphyrinato)europium(III) complexes with hydrophilic 15-crown-5 heads and hydrophobic alkyl or alkoxyphenyl tails, namely, $\text{Eu}_2[\text{Pc}(\text{15C5})_4]_2[\text{T}(\text{C}_{10}\text{H}_{21})_4\text{P}]$ (**1**) and $\text{Eu}_2[\text{Pc}(\text{15C5})_4]_2[\text{TPOPP}]$ (**2**) (Figure 1). In particular, these typical amphiphilic, sandwich, triple-decker molecules were fabricated

[a] Department of Chemistry, Shandong University
Jinan 250100, China
Fax: +86-531-8856-5211
E-mail: jzjiang@sdu.edu.cn

[b] University of Jinan
Jinan 250022, China

[c] Department of Chemistry, University of Jining
Qufu 273155, China

Supporting information for this article is available on the WWW under <http://www.eurjic.org/> or from the author.

into OFET devices by the Langmuir–Blodgett (LB) technique after surface treatment for the SiO₂/Si substrates, which show good carrier mobilities as high as 0.78 cm²V⁻¹s⁻¹ for holes. The present work not only develops a new series of sandwich-type tetrapyrrole rare-earth complexes as novel organic semiconductors but more importantly represents part of the new efforts towards knowing more about the relationship between molecular structure, film structure and OFET functional properties.

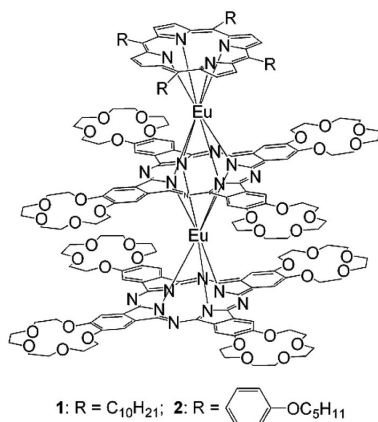


Figure 1. Schematic molecular structures for mixed (phthalocyaninato)(porphyrinato)europium triple-decker complexes **1** and **2**.

Results and Discussion

Synthesis

Metal-free porphyrins with four 4-pentyloxyphenyl and *n*-decyl groups at the *meso* positions of the porphyrin ring, H₂TPOPP and H₂T(C₁₀H₂₁)₄P, were prepared according to literature procedures.^[13,14] Mixed (phthalocyaninato)(porphyrinato)europium triple-decker complexes Eu₂[Pc(15C5)₄]₂[T(C₁₀H₂₁)₄P] (**1**) and Eu₂[Pc(15C5)₄]₂[TPOPP] (**2**) were synthesized and purified by the raise-by-one-story process by using Eu(acac)₃·H₂O, Eu[Pc(15C5)₄]₂ and H₂T(C₁₀H₂₁)₄P/H₂(TPOPP) as starting materials in refluxing 1,2,4-trichlorobenzene (TCB).^[15] Satisfactory elemental analysis results were obtained for both the newly prepared heteroleptic amphiphilic europium triple-decker complexes **1** and **2**, which have good solubility in common organic solvents such as CHCl₃, CH₂Cl₂ and toluene, after repeated column chromatography and recrystallization. These two triple-decker complexes were also characterized by MALDI-TOF mass spectrometry and ¹H NMR spectroscopy.

Spectroscopic Characteristics

The electronic absorption spectra of mixed-ring europium triple-deckers **1** and **2** in the region of 250–1000 nm were recorded in chloroform and the data are summarized in Table 1. The spectra are analogous to those reported for related (phthalocyaninato)(porphyrinato) rare-earth triple-

decker compounds and thus can be assigned in a similar manner.^[16] For compounds **1** and **2**, all the Soret and Q absorption bands experience a redshift when compared with those of their unsubstituted phthalocyaninato analogues. This can be attributed to the electron-donating properties of tetra(15-crown-5) substituents at the phthalocyanine ring(s). Similar phenomena have also been observed for alkyl- or alkoxy-substituted phthalocyanine-containing sandwich compounds.^[15,16] It is worth noting that the porphyrin Soret band is also shifted in the red direction, indicating the existence of π–π interactions among the Por and Pc(15C5)₄ ligands in these two sandwich compounds. This was also established previously through systematic investigation of the electronic absorption and electrochemical properties over a series of mixed (porphyrinato)[(na)phthalocyaninato] rare-earth sandwich complexes.^[16,17]

Table 1. Electronic absorption spectroscopic data for triple-decker complexes **1** and **2** in chloroform.

Compound	λ_{\max} (nm) / log ϵ						
1	292 /	368 /	423 /	527 /	586 /	627 /	743 /
	5.00	5.19	4.85	4.53	4.49	4.83	4.48
2	293 /	366 /	421 /	490 /	526 /	622 /	727 /
	4.81	5.01	4.88	4.21	4.26	4.62	4.37

The ¹H NMR spectra of newly prepared triple-decker compounds **1** and **2** were recorded in CDCl₃ at room temperature. Figures S1 (Supporting Information) exhibits the ¹H NMR spectrum of compound **1** in CDCl₃. Two singlet signals appearing in the low-field region at 12.15 and 9.68 ppm are obviously due to the α protons of the two Pc rings, respectively. One singlet signal appearing in the high-field region at 3.25 ppm is obviously due to the α protons of the Por ring of triple-decker compound **1**. The signals for the aliphatic protons from the 15-crown-5 ether substituents are observed in the range 6.66–4.16 ppm and the alkyl side chains are in the range 1.05–0.38 ppm.

For heteroleptic tris(phthalocyaninato)(porphyrinato)europium compounds **1** and **2**, the characteristic phthalocyanine dianion IR bands for [Pc(15C5)₄]²⁻ at ca. 1354 cm⁻¹ attributed to the symmetric C–H bending of the CH₃ groups in the side chains of the phthalocyanine rings together with the isoindole stretching vibrations were observed in their spectra.^[18] The intense absorption bands observed at ca. 933 and 1200 cm⁻¹ are attributed to symmetric and asymmetric C–O–C stretching, respectively. The intense absorption bands at ca. 2864 (symmetric), 2927 (antisymmetric) and 3071 cm⁻¹ (symmetric) in the IR spectra are attributed to the C–H stretching vibrations of the CH₂ and CH₃ groups of the side chains, respectively.

Electrochemical Properties

The electrochemical behaviour of both triple-decker complexes was investigated by cyclic voltammetry (CV) and differential pulse voltammetry (DPV) in CH₂Cl₂. These triple-decker compounds display four one-electron oxi-

dations labelled as Oxd₁ through Oxd₄ and two one-electron reductions labelled Red₁ and Red₂ within the electrochemical window of CH₂Cl₂ under the present conditions. The separation between the reduction and oxidation peak potentials for each process is 65–90 mV. All these processes are attributed to successive removal from, or addition of one electron to, the ligand-based orbitals, as the oxidation state of the central trivalent europium ions in the triple-decker complexes does not change. The half-wave redox potential values vs. SCE are summarized in Table 2. A typical representative cyclic voltammogram and differential pulse voltammogram for **1** are displayed in Figure 2.

Table 2. Half-wave redox potentials of triple-decker complexes **1** and **2** in CH₂Cl₂ containing 0.1 M TBAP.

Com-pound	Oxd ₄	Oxd ₃	Oxd ₂	Oxd ₁	Red ₁	Red ₂ ^[a]	$\Delta E^{o}_{1/2}$ ^[b]
1	1.37	1.04	0.60	0.20	-0.84	-1.23	1.04
2	1.31	1.11	0.66	0.22	-0.89	-1.27	1.11

[a] Recorded by DPV. [b] $\Delta E^{o}_{1/2}$ is the potential difference between the first oxidation and first reduction processes, that is, the HOMO–LUMO gap of the corresponding molecule.

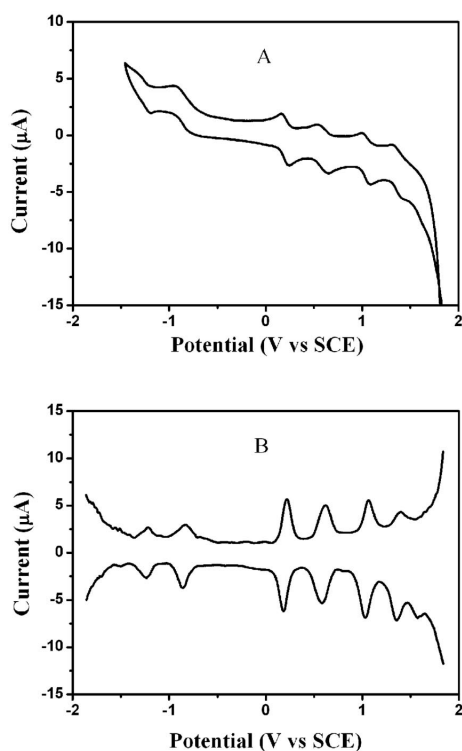


Figure 2. Cyclic voltammogram (A) and differential pulse voltammogram (B) of compound **1** in CH₂Cl₂ containing 0.1 M [Bu₄N]⁺[ClO₄⁻] at a scan rate of 20 and 10 mV S⁻¹, respectively.

The energy levels of the LUMO and HOMO can be obtained by the cyclic voltammetric measurement.^[19] The voltammogram of compounds **1** and **2** over the range of +1.5 to -2.0 V exhibited five coupled peaks of oxidation and reduction, respectively. The potential of the first ring reduction and the first ring oxidation is related to an energy level of its LUMO and HOMO.^[20] Thus, from the CV data,

the HOMO of compounds **1** and **2** can be approximated about -5.12 eV and -5.14 eV, respectively, which matches the work function of gold (5.1 eV). Therefore, a low-contact resistance is expected, which is likely to result in good Ohmic hole injection from the source electrode into the semiconductor.^[21]

Film Characterization and OFET Properties

Reproducible pressure–surface area (π - A) isotherms for **1** and **2** indicate that both compounds can form a stable monolayer on the surface of pure water as a result of their typical amphiphilic properties (Figure 3). The limiting molecular area obtained by extrapolation of the liquid-condensed phase to surface pressure zero is 5.06 and 3.64 nm² for **1** and **2**, respectively. These values are much smaller than the area of a phthalocyanine ring substituted with four 15-crown-5 moieties (6.25 nm²) calculated according to the PCMODEL program.^[22] This suggests that triple-decker molecules take an “edge-on” orientation on the water surface. This result is in good agreement with that of analogues (Pc)Dy[Pc(OC_nH_{2n+1})₈]Dy(Pc) ($n = 4, 8, 16$)^[23] as well as M(Pc)[Pc(OC₈H₁₇)₈] (M = Tb, Lu).^[24] These monolayers were transferred to hydrophobic substrates by the vertical dipping method and Z-type LB films were revealed to form for both triple-decker compounds.^[25] The fact that the transfer ratio was maintained at an ideal value of 1 during the whole transfer process clearly indicates the formation of uniform thin films with a very good layered structure (Figure S4, Supporting Information).

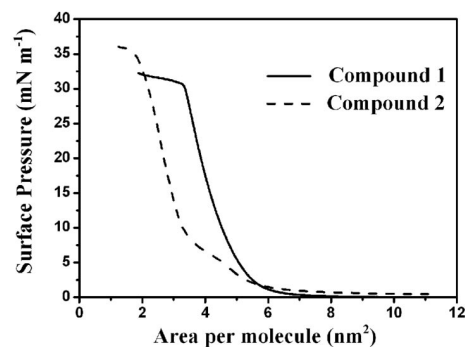


Figure 3. π - A isotherms of compounds **1** and **2** on a water surface at room temperature.

The orientation angles (dihedral angle between the phthalocyanine rings and the surface of the substrate) of the phthalocyanine ring in these films were determined by the polarized absorption spectroscopic method.^[26] The results are about 20.8 and 39.5° for **1** and **2**, respectively. Table S1 (Supporting Information) further confirms the “edge-on” configuration for the molecules in the film deduced from the π - A isotherms.

The low-angle X-ray diffraction experimental results of LB films for compound **2** show one diffraction peak corresponding to the d spacing of one layer as 3.04 nm (Figure S5, Supporting Information), which is similar to the calculated monolayer thickness 3.13 nm based on the orienta-

tion angle, the length of the side chains and the dimension of the molecule.^[23] In contrast, no diffraction peak was obtained from the low-angle X-ray diffraction experiment for the LB films of compound **1**, implying a molecular packing distorted from the longitudinal direction in multilayer films.^[27]

Figure 4 displays the UV/Vis spectra of these two mixed-ring triple-decker complexes in comparison with those in the LB films. In line with that of analogous $M_2(\text{Pc})_2\text{-}(\text{TCIPP})$ ($M = \text{Nd, Gd, Dy}$),^[28] the absorptions of triple-decker compound **1** in solution at about 292, 368 and 423 nm can be attributed to the phthalocyanine and porphyrin Soret bands, whereas the absorptions at 527, 586, 627 and 743 nm can be attributed to their Q bands. In the LB films, the corresponding absorptions of compound **1** are observed at 297, 366, 415, 506, 579, 633 and 750 nm. In comparison to that in solution, the absorption spectrum of the LB film given in Figure 4A shows either redshifted components from 292, 627, 743 to 297, 633, 750 nm, respectively, or blueshifted components from 368, 423, 527, 586 to 366, 415, 506, 579 nm, respectively. This is also true for triple-decker **2** (Figure 4B). The point-dipole model of Kasha provides a rationale for the observed band shifts. The extreme cases are represented by a head-to-tail arrangement of the dipoles, which results in a redshifted absorption band (*J* aggregate), and a parallel arrangement of the dipoles (*H* aggregate) with a blueshifted absorption band.^[29] The red- and blueshifted band components observed in the present case for LB films of triple-decker complexes **1** and **2** represent an intermediate case.^[30] The triple-decker molecules in LB films take a “face-to-face” conformation and “edge-on” orientation, in line with the behaviour of their π -*A* isotherms, as discussed above. The foregoing findings supports the viewpoint that the packing mode of the molecular assemblies constructed in the LB films of these two mixed-ring triple-decker complexes is similar to each other. This is also consistent with the polarized UV/Vis absorption spectroscopic result as detailed above. It is worth noting that effective intramolecular π - π stacking in the triple-decker molecules themselves provides the π electrons (as

well as holes) with an extensive area for delocalization. This forms the basic necessary characteristic for an organic semiconductor with good carrier mobility.^[31]

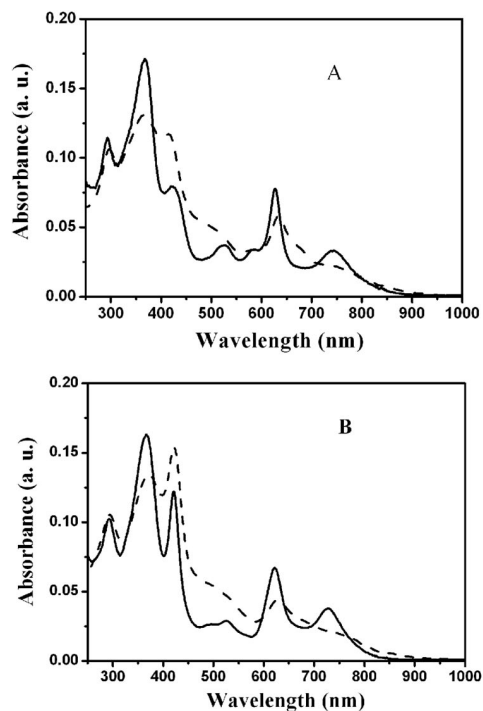


Figure 4. Electronic absorption spectra of compounds **1** (A) and **2** (B) in solution (solid line) and in LB film (dashed line).

The LB films were also characterized by atomic force microscopy (AFM). Figure 5 displays the height images of the 10-layer LB film of $\text{Eu}_2[\text{Pc}(15\text{C}5)_4]_2[\text{T}(\text{C}_{10}\text{H}_{21})_4\text{P}]$ (**1**) on hexamethyldisilazane (HMDS)-treated and octadecyltrichlorosilane (OTS)-treated SiO_2/Si surfaces. The scan in Figure 5A shows that the film formed on the HMDS-treated SiO_2/Si surface consists of a high density of small grains approximately 50 nm in size. In contrast, Figure 5B shows that the connectivity and order of the film of compound **1** formed on the OTS-treated SiO_2/Si surface is relatively

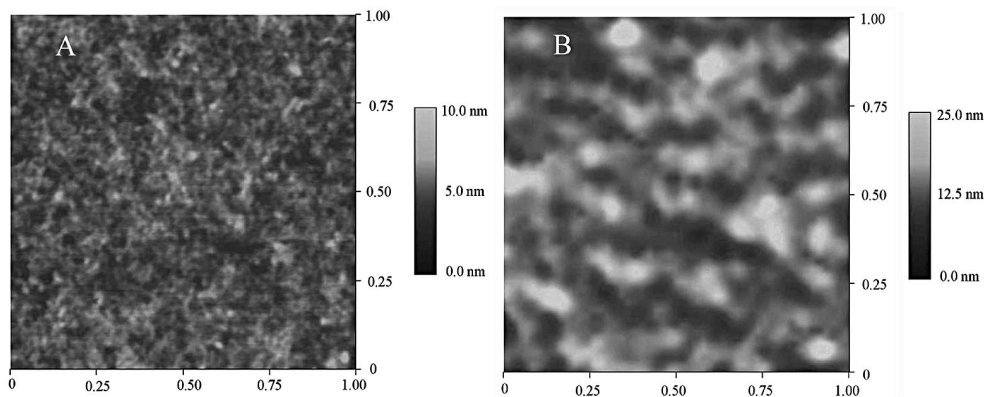


Figure 5. AFM topography images of the 10-layer film of compound **1**: deposited on HMDS-treated SiO_2/Si substrate; scan range: $1 \times 1 \mu\text{m}^2$; height: 0–15 nm; tapping mode (A); deposited on OTS-treated SiO_2/Si substrate; scan range: $1 \times 1 \mu\text{m}^2$; height: 0–35 nm; tapping mode (B).

poor. As expected, the uniform size of aggregates should reduce the boundaries and carrier traps in the film formed on the HMDS-treated SiO₂/Si surface and results in improved carrier mobility as detailed below. Comparison of the AFM images reveals the significant influence of the treatment of the substrate surface on the molecular packing in LB films. This is also true for triple-decker analogue **2**. As displayed in Figure S3 (Supporting Information), the connectivity and order of the LB film for triple-decker compound **2** on the HMDS-treated SiO₂/Si surface is better than those on the OTS-treated SiO₂/Si surface.

The devices fabricated from the LB films with top contact configuration show typical *p*-channel characteristics, as exemplified in Figures 6 and S6–S8 (Supporting Information). We calculated the carrier mobility (μ) by using the saturation region transistor equation, $I_{ds} = (W/2L)\mu C_0(V_G - V_T)^2$, where I_{ds} is the source-drain current, V_G the gate voltage, C_0 the capacitance per unit area of the dielectric layer and V_T the threshold voltage.^[32] The results indicate that both triple-decker compounds show good carrier mobility and on/off ratio. In addition, the OFET performance was found to be affected by the structure of the side chains and the treatment of the substrate. The devices fabricated from triple-decker compound **1** on the HMDS-treated SiO₂/Si substrate presents the largest carrier mobility for holes of 0.78 cm²V⁻¹s⁻¹ with an on/off ratio of 2.20 × 10⁴ and a threshold voltage of about -3.84 V (Figure 6). In line with the film morphology investigation result, application of the OTS-treated SiO₂/Si substrate diminishes the carrier mobility to 0.04 cm²V⁻¹s⁻¹ with an on/off ratio of

4.94 × 10³ and threshold voltage of about -4.02 V (Figure S6, Supporting Information). The devices fabricated from triple-decker **2** by using the HMDS-treated SiO₂/Si substrate show carrier mobility in the order of 0.05 cm²V⁻¹s⁻¹ with an on/off ratio of 1.48 × 10⁴ (Figure S7, Supporting Information) and a threshold voltage of about -1.19 V. Surface treatment with the OTS-treated SiO₂/Si substrate led to a decrease in the OFET performance of the same compound with the carrier mobility of 0.03 cm²V⁻¹s⁻¹, on/off ratio of 1.03 × 10⁴ and threshold voltage of about -4.34 V (Figure S8, Supporting Information). In addition, the threshold voltages for the devices fabricated from both triple-decker mixed-ring complexes are very low. It is noteworthy that a low threshold voltage is one of the basic requirements for developing practical applications of OFETs, especially for low-power applications.

Conclusions

In summary, two new mixed (phthalocyaninato)(porphyrinato)europium triple-decker sandwich complexes with hydrophilic 15-crown-5 heads and hydrophobic alkyl or pentyloxyphenyl tails were developed as novel organic semiconductors. The OFET devices fabricated from these mixed-ring sandwich complexes by the LB technique show good carrier mobility for holes. The present work, representing a new effort towards knowing the information between molecular structure, film structure and OFET functional properties, sheds further light on devising and preparing molecular materials for OFET devices and in particular for understanding the relationship between molecular structure and OFET functional properties.

Experimental Section

Measurements: ¹H NMR spectra were recorded with a Bruker DPX 300 spectrometer (300 MHz) in CDCl₃ by using the residual solvent resonance of CHCl₃ at $\delta = 7.26$ ppm relative to SiMe₄ as internal reference. Electronic absorption spectra were recorded with a Hitachi U-4100 spectrophotometer. MALDI-TOF mass spectra were taken with a Bruker BIFLEX III ultra-high-resolution Fourier transform ion cyclotron resonance (FTICR) mass spectrometer with α -cyano-4-hydroxycinnamic acid as the matrix. Elemental analyses were performed by the Institute of Chemistry, Chinese Academy of Sciences. Electrochemical measurements were carried out with a BAS CV-50W voltammetric analyzer. The cell comprised inlets for a glassy carbon disk working electrode of 3.0 mm in diameter and a silver-wire counter electrode. The reference electrode was Ag/Ag⁺ (0.01 mol dm⁻³), which was connected to the solution by a Luggin capillary, whose tip was placed close to the working electrode. It was corrected for junction potentials by being referenced internally to the ferrocenium/ferrocene (Fc⁺/Fc) couple [$E_{1/2}$ (Fc⁺/Fc) = 0.50 V vs. SCE]. Typically, a 0.1 mol dm⁻³ solution of [Bu₄N][ClO₄] in CH₂Cl₂ containing 0.5 mmol dm⁻³ of sample was purged with nitrogen for 10 min, then the voltammograms were recorded at ambient temperature. The scan rate was 20 and 10 mV s⁻¹ for CV and DPV, respectively.

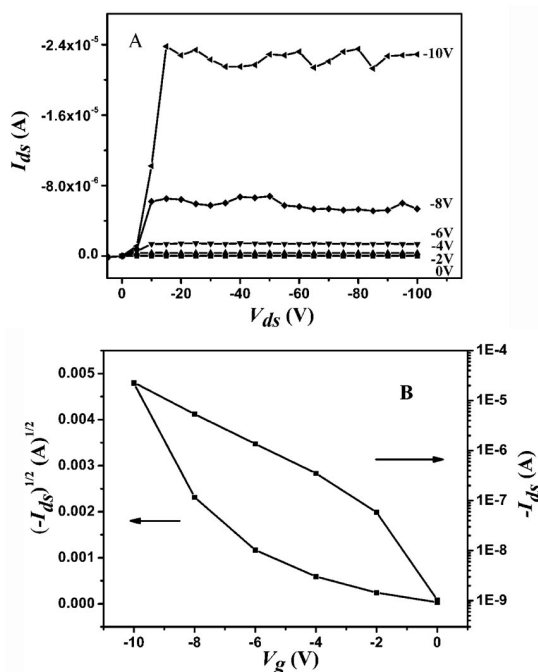


Figure 6. Drain-source current (I_{ds}) vs. drain-source voltage (V_{ds}) characteristic at different gate voltage (A) and transfer characteristic at $V_{ds} = -100$ V (B) for the OFET of compound **1** on the HMDS-treated SiO₂/Si substrate.

Thin-Film Deposition and Characterization: A solution of [Pc-(15C5)₄]Eu[Pc(15C5)₄] Eu(Por) dissolved in CH₂Cl₂ (1.46×10^{-5} to 1.59×10^{-5} mol L⁻¹) was spread onto ultra-pure water (resistivity: 18 MΩ cm⁻¹, pH 6.4) subphase surface. The monolayer properties were studied by measuring pressure–area isotherms with a NIMA SYSTEM 622 LB trough (Great Britain). All LB films were deposited onto hydrophobic quartz plates by the vertical dipping method with a dipping speed of 8 mm min⁻¹ while the surface pressure was kept at 22 mN m⁻¹. UV/Vis spectra and polarized UV/Vis spectra for the films were recorded with a Hitachi U-4100 spectrophotometer. Low-angle X-ray diffraction (LAXD) experiments were carried out with a Rigaku D/max-γB X-ray diffractometer. Morphology examination was carried out with a Veeco Nanoscope Multimode III SPM with tapping mode.

OFET Device Fabrication: The heavily doped silicon layer functioning as the gate electrode and the source/drain electrodes were thermally evaporated onto the LB films by use of a shadow mask. These electrodes have a width (*W*) of 28.6 mm and a channel length (*L*) of 0.24 mm. The ratio of the width to length (*W/L*) of the channel was then 119. The oxide layer of 5000 Å is the gate dielectric having a capacitance per unit area of 10 nF cm⁻². Before depositing the LB films, surface treatment for SiO₂/Si substrates was performed according to a literature method by using HMDS and OTS, respectively, as detailed below.^[33] The electric characteristics of these devices were measured in air. The current–voltage characteristics were obtained with a Hewlett–Packard (HP) 4140B parameter analyzer at room temperature.

A drop of HMDS was added to the cell culture dish (90 mm), which contained cleaned SiO₂/Si substrates. Then, the cell culture dish was put into an airtight vial overnight. After being taken out, the substrates were rinsed with chloroform and methanol to remove the redundant HMDS. To treat the substrates with OTS, cleaned SiO₂/Si substrates were placed in a flask under an atmosphere of nitrogen, which contained one drop of OTS. The flask was heated at 120° for 3 h in vacuo. After being cooled to room temperature, the substrates were rinsed with chloroform and methanol, and then ultrasonically cleaned with hexane for 15 min to remove the residual organic contamination and then dried with nitrogen.

Chemicals: Anhydrous 1,2,4-trichlorobenzene, hexamethyldisilazane and octadecyltrichlorosilane were purchased from Aldrich. Dichloromethane for voltammetric studies was freshly distilled from CaH₂ under an atmosphere of nitrogen. Column chromatography was carried out on silica gel (Merck, Kieselgel 60, 70–230 mesh) with the indicated eluents. All other reagents and solvents were used as received. The compounds Eu(acac)₃·H₂O,^[34] H₂T(C₁₀H₂₁)₄P,^[14] H₂TPOPP^[13] and Eu[Pc(15C5)₄]₂^[35] were prepared according to their published procedures.

meso-5,10,15,20-Tetra-*n*-decylporphyrin: Pyrrole (0.35 mL, 5.0 mmol) and undecanal (1.1 mL, 5.0 mmol) were combined in chloroform (500 mL). After purging the solution for 45 min with nitrogen, trifluoroacetic acid (0.20 mL) was added. The mixture was stirred under an atmosphere of nitrogen in the absence of light for 25 h before DDQ (0.86 g, 3.8 mmol) was added. The solution was evaporated under reduced pressure, and the residue was chromatographed on a silica gel column (CHCl₃/hexane, 1:4). Repeated chromatography followed by recrystallization from CHCl₃ and MeOH gave the pure target compound as a red-brown compound. Yield: 310 mg (31%). ¹H NMR (300 MHz, CDCl₃): δ = 9.45 (s, 8 H, Por ring), 4.89–4.94 (m, 8 H, CH₂ of alkyl), 2.51 (m, 8 H, CH₂ of alkyl), 1.75–1.85 (m, 8 H, CH₂ of alkyl), 1.28–1.52 (m, 48 H, CH₂ of alkyl), 0.85–0.88 (m, 12 H, CH₂ of alkyl), –2.64 (s, 2 H, Por ring) ppm. MS (MALDI-TOF): *m/z* = 872.1 (an isotopic cluster

peaking). C₆₀H₉₄N₄·CHCl₃ (990.8): calcd. C 81.09, H 10.93, N 6.20; found C 81.46, H 10.18, N 6.06.

General Procedure for the Preparation of Eu₂[Pc(15C5)₄]₂-[T(C₁₀H₂₁)₄P] (1) and Eu₂[Pc(15C5)₄]₂[TPOPP] (2): A mixture of Eu(acac)₃·H₂O (95 mg, ca. 0.2 mmol) and H₂Por (0.08 mmol) in TCB (6 mL) was stirred for 4 h under a slow stream of nitrogen. After being cooled to room temperature, Eu[Pc(15C5)₄]₂ (35 mg, 0.013 mmol) was added, and the mixture was then heated at reflux for a further 18 h under an atmosphere of nitrogen. The residue left after removing the volatiles in vacuo was chromatographed on a silica gel column (CHCl₃). Unreacted H₂Por was eluted first. Then CHCl₃/MeOH (7%) was used to develop a black-green fraction containing the target triple-decker complex. Repeated chromatography followed by recrystallization from CHCl₃ and hexane gave pure compound as a dark powder.

Eu₂[Pc(15C5)₄]₂[T(C₁₀H₂₁)₄P] (1): Yield: 18 mg (38%). ¹H NMR (300 MHz, CDCl₃): δ = 12.15 (s, 8 H, Pc ring), 9.68 (br. s, 8 H, Pc ring), 6.53–6.66 (m, 16 H, CH₂ of crown ether), 5.94 (s, 8 H, CH₂ of crown ether), 5.50–5.56 (m, 16 H, CH₂ of crown ether), 5.10 (m, 8 H, CH₂ of crown ether), 4.84–4.86 (m, 16 H, CH₂ of crown ether), 4.76–4.78 (m, 16 H, CH₂ of crown ether), 4.61–4.65 (m, 32 H, CH₂ of crown ether), 4.16–4.21 (m, 16 H, CH₂ of crown ether), 3.25 (br. s, 8 H, Por ring), 0.94–1.05 (m, 48 H, CH₂ of alkyl), 0.82 (m, 12 H, CH₃ of alkyl), 0.67–0.70 (m, 16 H, CH₂ of alkyl), 0.38 (s, 8 H, CH₂ of alkyl) ppm. MS (MALDI-TOF): *m/z* = 3720.2 (an isotopic cluster peaking). C₁₈₈H₂₃₆Eu₂N₂₀O₄₀·CH₃OH (3752.0): calcd. C 59.12, H 6.22, N 7.29; found C 59.12, H 6.48, N 7.28.

Eu₂[Pc(15C5)₄]₂[TPOPP] (2): Yield: 20 mg (42%). ¹H NMR (300 MHz, CDCl₃): δ = 13.19 (s, 4 H, phenyl), δ = 12.15 (s, 8 H, Pc ring), 9.49 (br. s, 8 H, Pc ring), 3.29 (s, 8 H, Por ring), 9.29 (s, 4 H, phenyl), 6.43–6.46 (m, 4 H, phenyl), 4.65 (s, 4 H, phenyl), 6.58 (s, 8 H, CH₂ of crown ether), 6.35 (s, 8 H, CH₂ of crown ether), 5.84–5.89 (m, 8 H, CH₂ of crown ether), 5.42 (m, 16 H, CH₂ of crown ether), 5.05–5.10 (m, 16 H, CH₂ of crown ether), 4.87–4.92 (m, 8 H, CH₂ of crown ether), 4.72–4.83 (m, 16 H, CH₂ of crown ether), 4.42–4.65 (m, 32 H, CH₂ of crown ether), 4.18–4.33 (m, 16 H, CH₂ of crown ether), 2.41–2.46 (m, 8 H, CH₂ of pentyloxy), 2.02–2.19 (m, 8 H, CH₂ of pentyloxy), 1.84–1.96 (m, 8 H, CH₂ of pentyloxy), 1.34–1.39 (m, 12 H, CH₂ of pentyloxy), 1.27 (m, 8 H, CH₂ of pentyloxy), 0.86–0.91 (m, 4 H, CH₂ of pentyloxy) ppm. MS (MALDI-TOF): *m/z* = 3807.3 (an isotopic cluster peaking). C₁₉₂H₂₁₂Eu₂N₂₀O₄₄·1.5CHCl₃ (3986.8): calcd. C 58.29, H 5.40, N 7.03; found C 58.45, H 5.56, N 7.37.

Supporting Information (see also the footnote on the first page of this article): NMR spectra and 2D NMR experiments for **1**; AFM topography images of compound **2**; dipper area–time isotherms for compounds **1** and **2**; low-angle X-ray diffraction pattern of the LB film of compound **2**; drain–source current (*I_{ds}*) vs. drain–source voltage (*V_{ds}*) characteristic at different gate voltage and transfer characteristic for the OFET of compounds **1** and **2**; polarized UV/Vis spectroscopy of the LB films of compounds **1** and **2**.

Acknowledgments

Financial support from the Natural Science Foundation of China and Ministry of Education of China is gratefully acknowledged.

- [1] A. Tsumura, H. Koezuka, T. Ando, *Appl. Phys. Lett.* **1986**, *49*, 1210–1212.
- [2] a) C. D. Dimitrakopoulos, A. R. Brown, A. Pomp, *J. Appl. Phys.* **1996**, *80*, 2501–2508; b) C. D. Dimitrakopoulos, D. J.

- Mascaro, *IBM J. Res. Dev.* **2001**, *45*, 11–27; c) K. Xiao, Y. Q. Liu, G. Yu, D. B. Zhu, *Appl. Phys. A* **2003**, *77*, 367–370; d) C. Du, Y. Guo, Y. Liu, W. Qiu, H. Zhang, X. Gao, Y. Liu, T. Qi, K. Lu, G. Yu, *Chem. Mater.* **2008**, *20*, 4188–4190.
- [3] A. W. Snow, W. R. Barger in *Phthalocyanines Properties and Applications* (Eds.: C. C. Leznoff, A. B. P. Lever), VCH, New York, **1989**, vol. 1.
- [4] a) G. Guillaud, J. Simon, *Chem. Phys. Lett.* **1994**, *219*, 123–126; b) G. Guillaud, R. Chaabane, C. Jouve, M. Gamoudi, *Thin Solid Films* **1995**, *258*, 279–282; c) Z. Bao, A. J. Lovinger, A. Dodabalapur, *Appl. Phys. Lett.* **1996**, *69*, 3066–3068; d) J. Yuan, J. Zhang, J. Wang, X. Yan, D. Yan, W. Xu, *Appl. Phys. Lett.* **2003**, *82*, 3967–3969; e) J. Wang, X. Yan, Y. Xu, J. Zhang, D. Yan, *Appl. Phys. Lett.* **2004**, *85*, 5424–5426; f) K. Xiao, Y. Liu, Y. Guo, G. Yu, L. Wan, D. Zhu, *Appl. Phys. A* **2005**, *80*, 1541–1545.
- [5] R. Zeis, T. Siegrist, C. Kloc, *Appl. Phys. Lett.* **2005**, *86*, 22103/1–3.
- [6] Y. Y. Noh, J. J. Kim, Y. Yoshida, K. Yase, *Adv. Mater.* **2003**, *15*, 699–702.
- [7] a) S. Ito, T. Murashima, H. Uno, N. Ono, *Chem. Commun.* **1998**, 1661–1662; b) P. B. Shea, J. Kanicki, N. Ono, *J. Appl. Phys.* **2005**, *98*, 014503/1.
- [8] P. Checconi, G. Conte, S. Salvatori, R. Paolesse, A. Bolognesi, A. Berliocchi, F. Brunetti, A. D'Amico, A. Di Carlo, P. Lugli, *Synth. Met.* **2003**, *138*, 261–266.
- [9] a) K. Xiao, Y. Liu, X. Huang, Y. Xu, G. Yu, D. Zhu, *J. Phys. Chem. B* **2003**, *107*, 9226–9230; b) W. Hu, Y. Liu, Y. Xu, S. Liu, S. Zhou, D. Zhu, *Synth. Met.* **1999**, *104*, 19–26; c) Y. Liu, *Sensor and Actuators B: Chem.* **2001**, *80*, 202–207; d) S. Chen, Y. Liu, Y. Xu, Y. Sun, W. Qiu, X. Sun, D. Zhu, *Synth. Met.* **2006**, *156*, 1236–1240.
- [10] a) J. Jiang, D. K. P. Ng, *Acc. Chem. Res.* **2009**, *42*, 79–88; b) R. Li, P. Ma, S. Dong, X. Zhang, Y. Chen, X. Li, J. Jiang, *Inorg. Chem.* **2007**, *46*, 11397–11404; c) Y. Chen, W. Su, M. Bai, J. Jiang, X. Li, Y. Liu, L. Wang, S. Wang, *J. Am. Chem. Soc.* **2005**, *127*, 15700–15701; d) Y. Chen, R. Li, R. Wang, P. Ma, S. Dong, Y. Gao, X. Li, J. Jinag, *Langmuir* **2007**, *23*, 12549–12554; e) Y. Gao, P. Ma, Y. Chen, Y. Zhang, Y. Bian, X. Li, J. Jiang, C. Ma, *Inorg. Chem.* **2009**, *48*, 45–54.
- [11] a) Y. Bian, J. Jiang, Y. Tao, M. T. M. Choi, R. Li, A. C. H. Ng, P. Zhu, N. Pan, X. Sun, D. P. Arnold, Z.-Y. Zhou, H.-W. Li, T. C. W. Mak, D. K. P. Ng, *J. Am. Chem. Soc.* **2003**, *125*, 12257–12267; b) N. Pan, Y. Bian, M. Yokoyama, R. Li, T. Fukuda, S. Neya, J. Jiang, N. Kobayashi, *Eur. J. Inorg. Chem.* **2008**, *35*, 5519–5523.
- [12] a) J. Li, D. Gryko, R. B. Dabke, J. R. Diers, D. F. Bocian, W. G. Kuhr, J. S. Lindsey, *J. Org. Chem.* **2000**, *65*, 7379–7390; b) D. Gryko, J. Li, J. Diers, K. Roth, D. Bocian, W. Kuhr, J. Lindsey, *J. Mater. Chem.* **2001**, *11*, 1162–1180.
- [13] a) H. Zhao, J. Ning, Y. Lin, *Youji Huaxue* **2001**, *21*, 383–387; b) J. Ning, H. Zhao, N. Zhou, *Youji Huaxue* **2005**, *25*, 1381–1385.
- [14] M. A. Fox, J. V. Grant, D. Melamed, T. Torimoto, C.-Y. Liu, A. J. Bard, *Chem. Mater.* **1998**, *10*, 1771–1776.
- [15] a) T. Gross, F. Chevalier, J. S. Lindsey, *Inorg. Chem.* **2001**, *40*, 4762–4774; b) D. Chabach, A. De Cian, J. Fischer, R. Weiss, M. E. M. Bibout, *Angew. Chem. Int. Ed. Engl.* **1996**, *35*, 898–899.
- [16] a) J. Jiang, M. T. M. Choi, W. F. Law, J. Chen, D. K. P. Ng, *Polyhedron* **1998**, *17*, 3903–3908; b) J. Jiang, H. Yu, Y. Bian, *Acta Chim. Sinica* **1999**, *57*, 1285–1290; c) J. Jiang, J. Xie, M. T. M. Choi, Y. Yan, S. Sun, D. K. P. Ng, *J. Porphyrins Phthalocyanines* **1999**, *3*, 322–328; d) D. K. P. Ng, J. Jiang, *Chem. Soc. Rev.* **1997**, *26*, 433–442; e) M. Moussavi, A. De Cian, J. Fischer, R. Weiss, *Inorg. Chem.* **1986**, *25*, 2107–2108; f) T. H. Tran-Thi, T. A. Mattioli, D. Chabach, A. De Cian, R. Weiss, *J. Phys. Chem.* **1994**, *98*, 8279–8288; g) D. Chabach, M. Tahiri, A. De Cian, J. Fischer, R. Weiss, M. Bibout, *J. Am. Chem. Soc.* **1995**, *117*, 8548–8556; h) J. Jiang, T. C. W. Mak, D. K. P. Ng, *Chem. Ber.* **1996**, *129*, 933–936; i) J. Jiang, R. L. C. Lau, T. D. W. Chan, T. C. W. Mak, D. K. P. Ng, *Inorg. Chim. Acta* **1997**, *255*, 59–64; j) J. Jiang, W. Liu, W. F. Law, D. K. P. Ng, *Inorg. Chim. Acta* **1998**, *268*, 49–53.
- [17] N. Pan, J. Jiang, X. Cui, D. P. Arnold, *J. Porphyrins Phthalocyanines* **2002**, *6*, 347–357.
- [18] J. Jiang, M. Bao, L. Rintoul, D. P. Arnold, *Coord. Chem. Rev.* **2006**, *250*, 424–448 and references cited therein.
- [19] V. Parra, T. Del Caño, M. L. Rodríguez-Méndez, J. A. de Saja, R. F. Aroca, *Chem. Mater.* **2004**, *16*, 358–364.
- [20] P. Zhu, N. Pan, R. Li, J. Dou, Y. Zhang, D. Cheng, D. Wang, D. K. P. Ng, J. Jiang, *Chem. Eur. J.* **2005**, *11*, 1425–1432.
- [21] a) J. Zaumseil, H. Sirringhaus, *Chem. Rev.* **2007**, *107*, 1296–1323; b) J. Wang, H. Wang, X. Yan, H. Huang, D. Jin, J. Shi, Y. Tang, D. Yan, *Adv. Funct. Mater.* **2006**, *16*, 824–830; c) A. Babel, J. D. Wind, S. A. Jenekhe, *Adv. Funct. Mater.* **2004**, *14*, 891–898.
- [22] PCMODEL for Windows, version 6.0, Serena Software.
- [23] Y. Chen, H. Liu, P. Zhu, Y. Zhang, X. Wang, X. Li, J. Jiang, *Langmuir* **2005**, *21*, 11289–11296.
- [24] W. Su, J. Jiang, K. Xiao, Y. Chen, Q. Zhao, G. Yu, Y. Liu, *Langmuir* **2005**, *21*, 6527–6531.
- [25] a) Y. Chen, Y. Zhang, P. Zhu, Y. Fan, Y. Bian, X. Li, J. Jiang, *J. Colloid Interface Sci.* **2006**, *303*, 256–263; b) X. Wang, Y. Chen, H. Liu, J. Jiang, *Thin Solid Films* **2006**, *496*, 619–625; c) Y. Chen, H. Liu, N. Pan, J. Jiang, *Thin Solid Films* **2004**, *460*, 279–285.
- [26] a) M. Yoneyama, M. Sugi, M. Saito, K. Ikegama, S. Kuroda, S. Iizima, *Jpn. J. Appl. Phys.* **1986**, *25*, 961–965; b) N. Kobayashi, H. Lam, W. A. Nevin, P. Janda, C. C. Leznoff, T. Koyama, A. Monden, H. Shiral, *J. Am. Chem. Soc.* **1994**, *116*, 879–890.
- [27] a) F. Wurthner, *Chem. Commun.* **2004**, *14*, 1564–1579; b) K. Balakrishnan, A. Datar, T. Naddo, J. Huang, R. Oitker, M. Yen, J. Zhao, L. Zang, *J. Am. Chem. Soc.* **2006**, *128*, 7390–7398; c) P. M. Kazmaier, R. Hoffmann, *J. Am. Chem. Soc.* **1994**, *116*, 9684–9691; d) K. Balakrishnan, A. Datar, R. Oitker, H. Chen, J. Zuo, L. Zang, *J. Am. Chem. Soc.* **2005**, *127*, 10496–10497.
- [28] X. Sun, R. Li, D. Wang, J. Dou, P. Zhu, F. Lu, C. Ma, C.-F. Choi, D. Y. Y. Cheng, D. K. P. Ng, N. Kobayashi, J. Jiang, *Eur. J. Inorg. Chem.* **2004**, *19*, 3806–3813.
- [29] M. Kasha, H. R. Rawls, M. A. El-Bayoumi, *Pure Appl. Chem.* **1965**, *11*, 371–392.
- [30] M. J. Cook, I. Chambrier in *Porphyrin Handbook Vol 17 – Phthalocyanines: Properties and Materials* (Eds.: K. M. Kadish, K. M. Smith, R. Guilard), Elsevier, USA, **2003**, pp. 37–127.
- [31] H. E. Katz, Z. Bao, *J. Phys. Chem. B* **2000**, *104*, 671–678.
- [32] S. M. Sze, *Physics of Semiconductor Devices*, John Wiley & Sons, New York, **1981**.
- [33] H. Z. Chen, M. M. Ling, X. Mo, M. M. Shi, M. Wang, Z. Bao, *Chem. Mater.* **2007**, *19*, 816–824.
- [34] J. G. Sittes, C. N. McCarty, L. L. Quill, *J. Am. Chem. Soc.* **1948**, *70*, 3142–3143.
- [35] N. Sheng, R. Li, C.-F. Choi, W. Su, D. K. P. Ng, X. Cui, K. Yoshida, N. Kobayashi, J. Jiang, *Inorg. Chem.* **2006**, *45*, 3794–3802.

Received: November 21, 2008

Published Online: January 29, 2009